

Research Article

Multi-sensor points cloud data fusion for 3D building models: A case study in Halong City, Vietnam

Ha Thu Thi Le^{1,2*}

¹ Hanoi University of Mining and Geology, Hanoi, Vietnam; lethithuha@humg.edu.vn

² Geomatics in Earth Sciences Research Group, Hanoi University of Mining and Geology, Hanoi, Vietnam; lethithuha@humg.edu.vn

*Corresponding author: lethithuha@humg.edu.vn; Tel.: +84-983115967

Received: 28 April 2024; Accepted: 04 June 2024; Published: 25 September 2024

Abstract: Three-dimensional building models play a crucial role in urban planning, emergency response, disaster management, and decision-making. Multi-sensor data fusion has recently attracted significant interest in the Geomatics research community. This approach addresses the limitations of individual sensors, allowing for the creation of comprehensive 3D models of structures and improving object classification. This study focuses on developing approaches that combine various geospatial technologies to produce a complete 3D model of common urban architectures, including high building, neighboring villa, and individual home. This research used flexibly employ UAV aerial imagery, ground photography, and terrestrial LiDAR scanning to collect the necessary information for constructing complete 3D models of each characteristic urban structure. Different point cloud datasets will be processed, merged, and used to generate the completely 3D models. The experimental results have produced complete 3D models with accuracy achieved with Δx ; $m\Delta y$; $m\Delta z$ all below 10 cm for the experimental buildings. With the accuracy of the 3D models, it is entirely possible to achieve accuracy in horizontal plane and height for the 1:500 scale terrain map.

Keywords: 3D building models; Multi-sensor points data fusion; Halong city; Vietnam.

1. Introduction

Buildings are some of the most significant features in urban environments and are modeled for a range of uses, such as simulating air pollution, estimating energy use, detecting urban heat islands, and many other applications [1]. Three-dimensional (3D) building models play a crucial role in urban planning, emergency response, disaster management, and decision-making processes. 3D buildings aim to represent the geometry and appearance of reality, enabling us to see the city as it currently exists, how it appeared in the past, and how it is likely to appear in the future. Efficiently creating these models enhances digital library content concerning buildings and infrastructure and provides managers with essential tools for visualization and decision-making [2]. The concept of a three-dimensional (3D) model or representation is frequently linked to the future due to its status as an increasingly utilized and evolving technology [3]. Advanced technologies in recent years have enabled the creation of accurate and intricate 3D models for depicting buildings as they were constructed [4]. There are some different data acquisition techniques used to create the 3D object modeling: lidar, radar, camera (photogrammetry), and total stations [2, 5–7]. Images captured by drones are utilized to attain exceptionally detailed 3D models, enabling the reconstruction of both the geometry and texture of the examined objects [1, 8–10]. Drones are now extensively employed for data gathering and 3D reconstruction objectives.

The quality of the resulting 3D data significantly relies on factors such as the specifications of the sensors utilized, the setup of the photogrammetric network, and the outcomes of image orientation. The growing adoption of UAVs in surveying tasks is largely attributed to their lightweight design and affordability. UAVs, which are unmanned, reusable motorized devices, generally hover vertically at low altitudes just a few meters above objects [1, 11]. Moreover, through the implementation of UAV photogrammetry, UAVs can swiftly gather data and offer high-resolution aerial photographs. Subsequently, the gathered data can be employed to recreate the terrain of a model representing the research area, resulting in highly detailed 3D mapping and modeling. This process considers factors such as image overlap, scale adjustments, and flight altitude [12]. Scanning surveys offer an advantage in terms of time efficiency, as they are automated and capable of capturing numerous details in a single scan, minimizing the risk of overlooking any details. In the current development trend, 3D Laser Scanning technology (TLS - Terrestrial Laser Scanner) is becoming known and applied in surveying and inspecting structures, gradually replacing the aforementioned devices due to its higher accuracy than UAVs, as the scanner is fixed on the ground. The 3D Laser Scanning equipment has the capability to collect numerous point clouds in space, which capture the detailed surface shapes of objects. Each point in these clouds contains coordinate information (XYZ) and color parameters. Besides, ground-based digital camera is another low-cost data acquisition technique, which is currently used in 3D modeling applications [13–18]. Unfortunately, however, digital cameras are restricted by line-of-sight limitations. Consequently, it can be observed that each data acquisition method has its own strengths and weaknesses. Hence, the fusion of data emerges as a critical concern for generating accurate 3D object models [19–21].

In Vietnam, the government has determined that developing smart cities is the best choice to support the current urbanization and economic growth process. Quang Ninh province and Ha Long city are making significant progress to align with the Government's strategy and priorities for smart city development in Vietnam. When constructing comprehensive 3D information models for urban areas, it's crucial to consider the distinctive features of coastal cities in Vietnam, considering the specific conditions present in each locality throughout the country. Previous domestic studies have shown that researching the construction of 3D models for some urban construction projects by integrating geospatial technologies remains limited. Moreover, the majority of recent studies only utilize a single type of geospatial technology to collect 3D information of individual construction objects [22, 23]. There have been few studies describing the process of integrating geospatial technologies to build high-precision 3D models for complex and characteristic structures such as coastal urban areas in Vietnam.

This research focuses on two main goals: (1) To propose a process for applying geospatial technology in collecting 3D spatial information for characteristic construction objects in coastal urban areas; (2) To develop high-precision 3D models for characteristic construction objects in Ha Long city, Quang Ninh province. Vietnam encounters a new challenge when it comes to processing data from diverse sensor sources. Currently, research predominantly concentrates on managing data from a solitary technology type, like UAV or aerial Lidar, terrestrial Lidar, or ground-based stereophotography. Managing data from a single sensor source is considerably simpler than handling data from multiple sensor sources with differing resolutions. Consequently, this persists as a challenge in developing thorough 3D models for particular construction projects in Vietnam.

2. Materials and Method

2.1. Description of the study site

The experimental area is located in Bai Chay ward and Hung Thang ward, Ha Long city, Quang Ninh province, Vietnam (Figure 1a), primarily encompassing the high-end coastal

urban area developed by BIM Group. The urban area consists of individual villas and adjacent villas. Additionally, it includes internal transportation systems, water supply and drainage systems, and public facilities serving the community. There are also several high-rise buildings along the main roads, serving as residences, hotels, or office headquarters for various organizations.



Figure 1. The study site.

Phat Linh Hotel Ha Long is a 5-star luxury hotel, located at A9, Lot 1, Ha Long Marine Boulevard, Ha Long city, Quang Ninh Province (Figure 1a). Phat Linh Hotel is a tall as being at least 120 m, continuously habitable building having 25 floors (Figure 1b).

The individual building is the Hạ Long New Day 2 hotel, a 5-story structure with an area of approximately 70 m², located as shown in Figure 1 (yellow boundary). The area surrounding the building is quite open. Architecturally, the building has a simple design typical of small hotels, with the front featuring large glass windows on the first floor and smaller windows on the upper floors (Figure 1c).

The neighboring villa consists of two rows of 5-story houses facing away from each other, currently in the handover and usage phase. The architecture is characterized by square geometric shapes, numerous glass windows, and uniformity among the units (Figure 1d).

2.2. Methodology

The methodology of this study can be categorized into three phases: data acquisition, data processing, result and accuracy assessment (Figure 2).

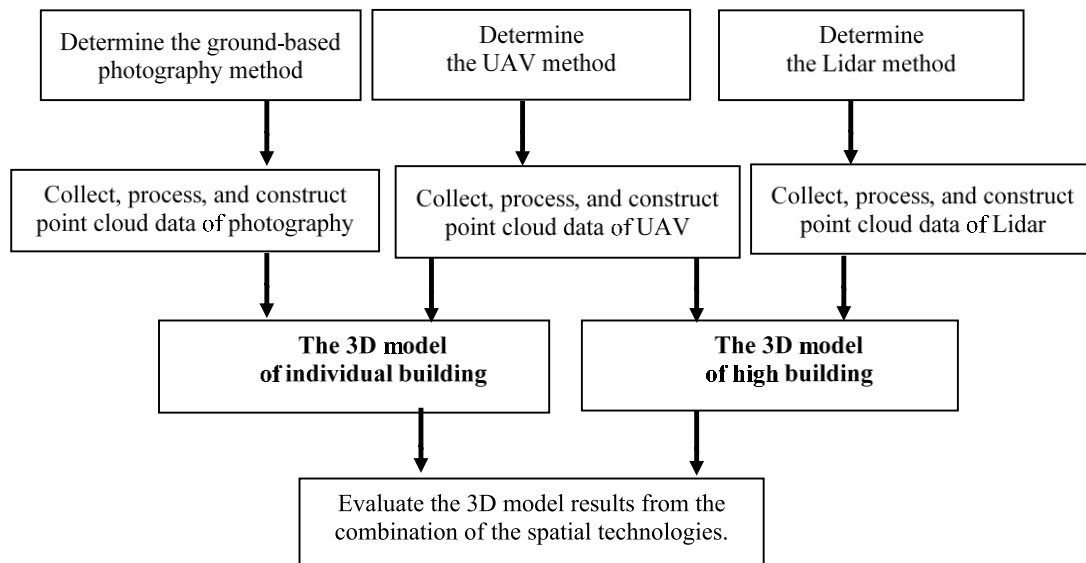


Figure 2. The flowchart of study.

2.2.1. Data acquisition

a) TLS data collection

FARO FOCUS^{3D} X130 TLS has been used as the main scanning system to capture point cloud data from different locations. During the field operation, 11 scans have been completed around the high building to capture the details of the building and create a good overlap between the scans (Figure 3a). FARO FOCUS^{3D} X130 has an integrated camera that allows the acquisition of the images needed to assign RGB values to every single point cloud.

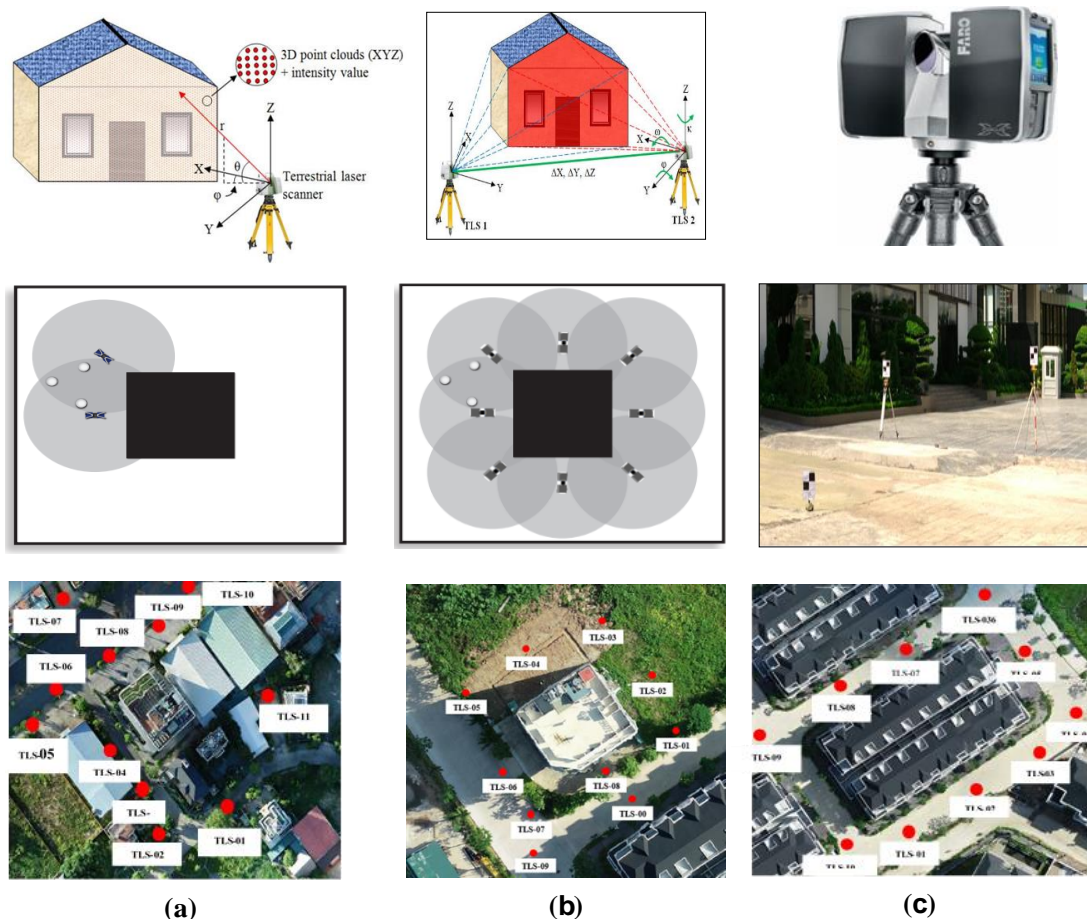


Figure 3. FARO FOCUS3D X130 TLS has been used to collect data.

b) UAV image acquisition

The UAS data acquisition has been performed using a low-cost DJI Phantom 4 Pro, in order to acquire a complete coverage of the building of interest, the flights have been planned and then executed for high building, individual building, and neighboring villa (Figure 4).



Figure 4. Data acquisition techniques by DJI Phantom 4 Pro V2.0.

c) Ground-Based digital camera data collection

The task of designing the photo capture route essentially involves arranging the digital photography stations. Based on the accuracy requirements, camera parameters, and the characteristics of the field, the parameters for each ground photo capture route for buildings are determined (Figure 5).

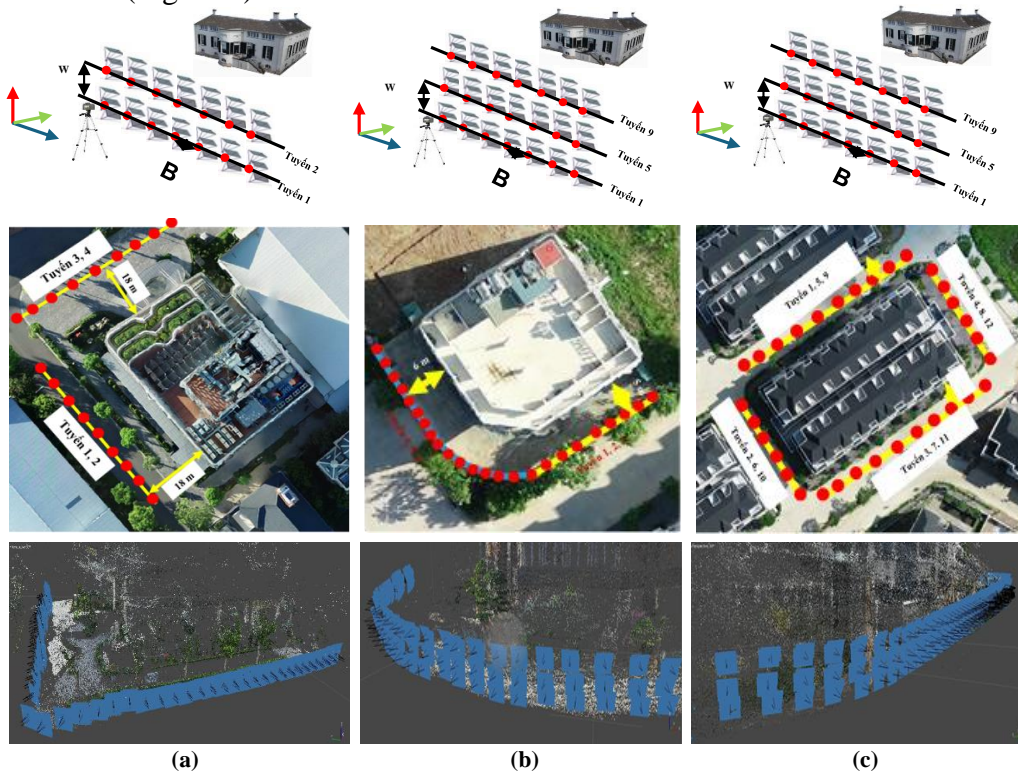


Figure 5. The collected data from the terrestrial camera (TC).

2.2.2. Data processing

Integration of point clouds from multi-sensor: To improve the accuracy of the point cloud after merging, the ICP method is used [24]. Before concatenation, the UAV, TC and TLS point clouds are filtered for noise (Figures 6, 7). Filter noise from point clouds to remove points of unimportant objects such as wires, trees, etc. or points that were wrong in previous processing. In addition, noise filtering also reduces the capacity of the point cloud. Because the TC and TLS point cloud have a higher density of points and higher accuracy, it is used as the base point cloud and the UAV point cloud is the composite point cloud.

The data concatenation process consists of two steps: Coarse Alignment and Fine Alignment. In which, in the raw coupling step, it is necessary to select at least 4 duplicate points on two points cloud. This can be a focal point, a control point, or a sharp feature on two points cloud. During the exact matching stage, there is a notable increase in the number of points involved in the matching process, resulting in enhanced accuracy of data matching albeit at the expense of longer processing time. The concatenation of point cloud data in both steps is executed using Cloudcompare software.

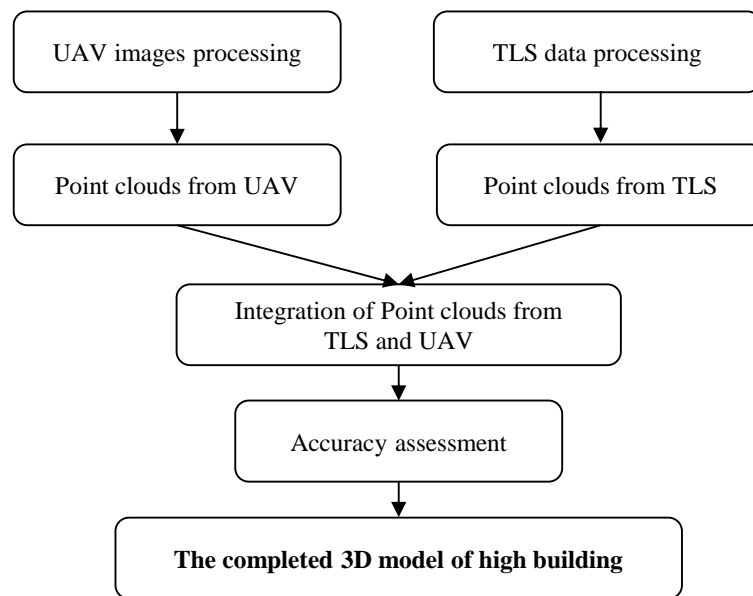


Figure 6. Flowchart in data processing phase for high building.

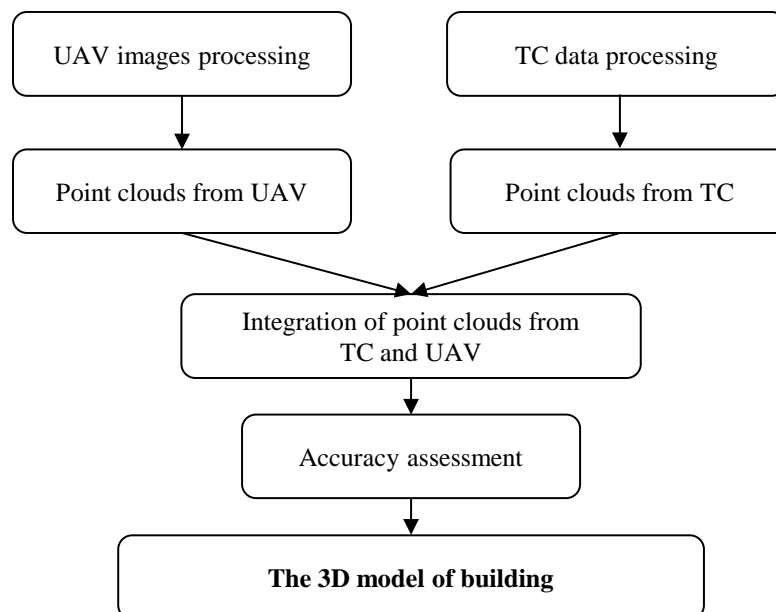


Figure 7. Flowchart in data processing phase for individual building and neighboring villa.

2.2.3. Accuracy assessment

To evaluate the accuracy of 3D point clouds integrating geospatial technologies of construction projects, it is necessary to arrange the above image control points on the surface and around high buildings and independent buildings, and adjacent villa area. The points are arranged evenly on all sides of the building, with the point layout diagram as shown below.

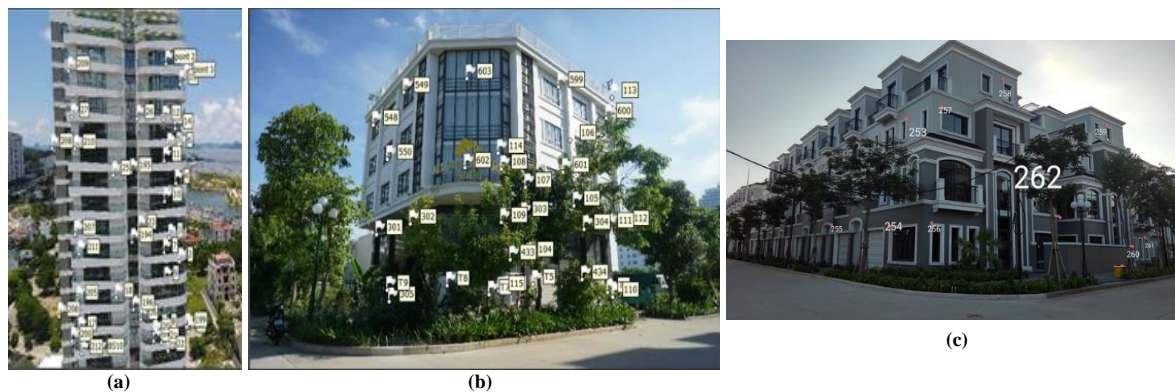


Figure 8. Distribution of image control points and checkpoints.

3. Results and discussion

3.1. Points cloud data of buildings

a) Point clouds from TLS data

The processing TLS data includes steps: (1) create project, (2) import data of scanning stations (Import), (3) process scan stations (Processing), (4) merge scan stations and evaluate accuracy (Registration), (5) create a cloud point cloud (Create point cloud), and export point cloud (Export).

With TLS data, scans are dumped in SCENE software, handling point clouds creation and station pairing. The result of the processing is point clouds as shown in Figure 9.



Figure 9. Point clouds from TLS data.

The data scanned from the FARO FOCUS3D X130 TLS device was transferred to a computer and processed using the SCENE software. The stations were aligned, and the accuracy was assessed, and the results were exported in E75 format. The outcome of the processing is point clouds as shown in Figures 9a-9c.

b) Point clouds from UAV images

UAV image data processed on the software is Agisoft Metashape. Software Agisoft uses SfM algorithms include steps: (1) Identify the above features image through using a special transformation algorithm multi-scale feature (SIFT); (2) Matching points featured; (3)

Orientation in and out of the image; (4) Creating dense point clouds. The result of the processing is point clouds as shown in Figure 10.

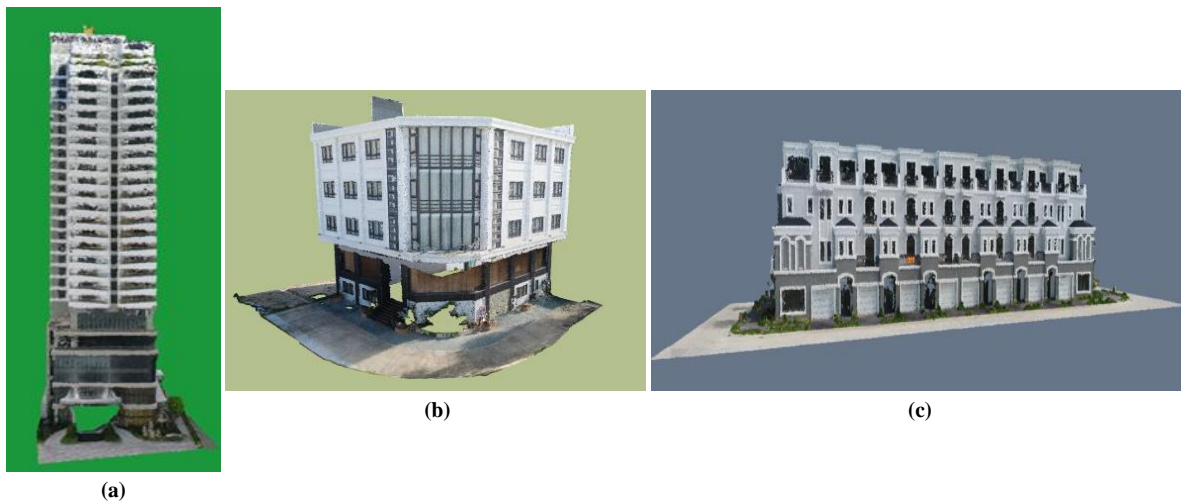


Figure 10. Point clouds from UAV data.

The creation of 3D models and processing of UAV images for high buildings, independent buildings, and adjacent villas were conducted using the specialized software Agisoft Metashape. This process yielded a dense point cloud for the high building, individual building, and adjacent villa, as illustrated in Figures 10a-10c.

c) Point clouds from terrestrial camera (TC) data

The terrestrial camera image data processed on the software is Agisoft Metashape. Software Agisoft uses SfM algorithms include steps: (1) Identify the above features image through using a special transformation algorithm multi-scale feature (SIFT); (2) Matching points featured; (3) Orientation in and out of the image; (4) Creating dense point clouds. The result of the processing is point clouds as shown in Figure 11.

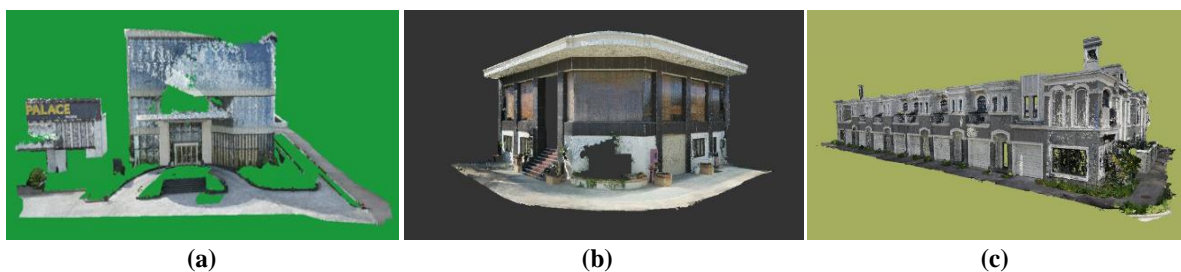


Figure 11. Point clouds from TC data.

Processing ground-based images and creating 3D models were conducted using the specialized image processing software Agisoft Metashape. The procedure was similar to processing UAV images. The result is a point cloud model of the high building, independent buildings, and adjacent villas, as shown in Figures 11a-11c.

3.2. Multi-sensor points cloud data fusion for 3D building models

a) Integration of point clouds from UAV and TLS for the high building

The iterative closest point (ICP) algorithm consistently converges monotonically to the nearest local minimum of a mean-square distance metric. Empirical evidence indicates that the convergence rate is especially fast in the initial iterations. Consequently, with an appropriate set of initial rotations and translations for a specific class of objects characterized by a certain “shape complexity”, it is possible to globally minimize the mean-square distance metric across all six degrees of freedom by evaluating each initial alignment (Figures 12-14).

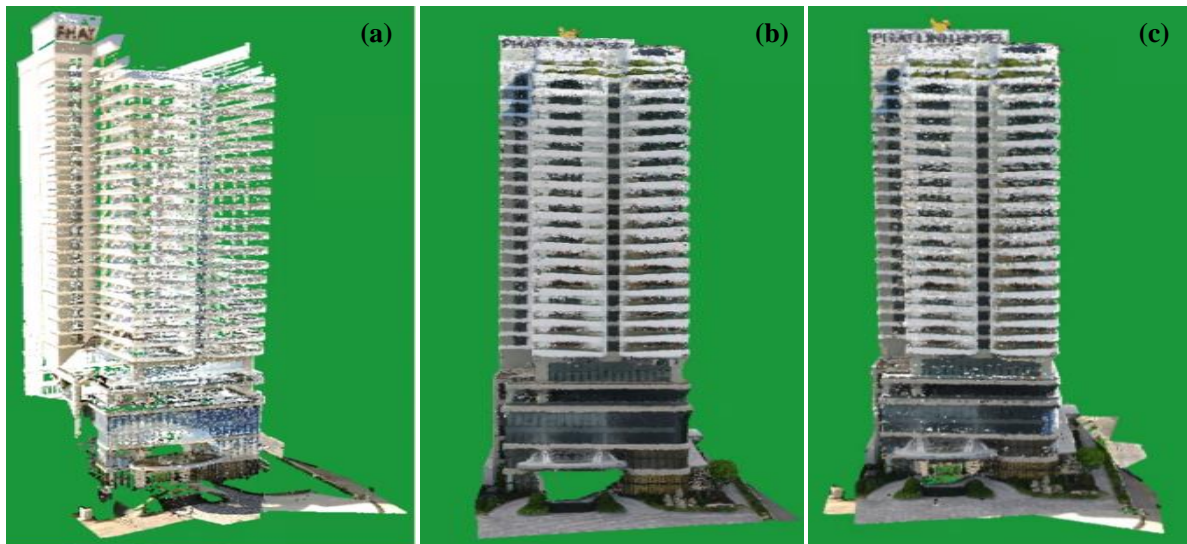


Figure 12. High building’s TLS point cloud after noise filtering (a), High building’s UAV point cloud after noise filtering (b), High building’s UAV and TLS point cloud after precision matching (c).

b) Integration of point clouds from UAV and TC for the independent building and neighboring villa



Figure 13. Independent building’s TC point cloud after noise filtering (a), Independent building’s UAV point cloud after noise filtering (b), Independent building’s UAV and TC point cloud after precision matching (c).



Figure 14. Neighboring villa’s TC point cloud after noise filtering (a), Neighboring villa’s UAV point cloud after noise filtering (b), Neighboring villa’s UAV and TC point cloud after precision matching (c).

3.3. Accuracy assessment

The reliability of these datasets was assessed by calculating the root mean square error (RMSE) between the coordinates of points on the generated orthophoto and those obtained from GPS measurements. A lower RMSE value signifies higher accuracy. The value of RMSE is shown in Tables 1-3.

Table 1. Results of assessing the accuracy of point clouds fusion from UAVs and TLS of high building.

No	M_x (cm)	M_y (cm)	M_p (cm)	M_h (cm)
3	-0.8	-0.8	1.1	0.9
6	0.4	-3.2	3.3	-1.7
18	4.4	-0.6	4.4	6.1
23	3.8	2.0	4.3	4.3
197	-2.3	-2.9	3.7	-0.9
203	-6.3	-1.9	6.5	-0.7
205	-5.9	-5.7	8.2	-2.4
212	-2.0	4.4	4.8	-19.5
RMSE	3.8	3.1	5.0	7.5

The results of assessing the accuracy of point clouds fusion from UAVs and TLS of high building are presented in Table 1. The root mean square errors are $m\Delta x = 3.8$ cm; $m\Delta y = 3.1$ cm; $m\Delta z = 5.0$ cm. With the accuracy of the checkpoints as shown in Tables 1, the 3D model can fully achieve high accuracy.

Table 2. Results of assessing the accuracy of point clouds fusion from UAVs and TC of independent building.

No	M_x (cm)	M_y (cm)	M_p (cm)	M_h (cm)
599	-0.36006	-1.08958	1.14753	-2.3491
107	0.187597	0.561629	0.592132	0.46285
105	-0.26855	0.225359	0.350582	0.238866
549	-1.3453	-2.81343	3.118529	-0.76773
RMSE	0.715331	1.53857	1.69673	1.26283

Table 3. Results of assessing the accuracy of point clouds fusion from UAVs and TC of neighboring villa.

No	M_x (cm)	M_y (cm)	M_p (cm)	M_h (cm)
244	-0.5	1.1	1.2	1.9
245	-0.7	1.6	1.7	4.0
246	-0.3	-2.7	2.7	2.8
267	-0.7	0.3	0.7	-0.2
269	-1.3	-0.8	1.5	-1.3
276	-1.8	-1.1	2.1	-0.3
206	0.4	-0.5	0.7	0.2
209	2.1	0.4	2.1	-0.9
211	0.4	-0.4	0.6	3.2
212	0.9	-1.7	1.9	-1.3
RMSE	1.4	1.3	1.7	2.1

The results of assessing the accuracy of point clouds fusion from UAV and TP technologies for independent building and adjacent villa rows are presented in Tables 2 and 3. Based on the coordinate measurements (x, y, z) of the characteristic points on the terrain, including door and building corner angles (in Figures 8b, c), directly on the 3D model of the point cloud obtained after processing the image capture results, and used for comparison with the coordinate measurements (x, y, z) of the corresponding characteristic points measured by the non-prism mode of the total station. With the accuracy of the checkpoints as shown in Table 2, Table 3, the 3D model can fully achieve accuracy in terms of the horizontal plane and height for the 1:500 scale topographic map.

3.4. Discussion

From the results of the 3D point clouds and the assessment process of the accuracy of the merged point clouds from different technologies, it is evident that this integration process has generated complete point clouds, each technology exhibiting its own advantages and

disadvantages. Each device allows for the measurement and representation of a portion of the object (e.g., independent building). Therefore, a solution combining devices and technologies to fully measure and represent an object needs to be proposed, tailored to specific cases as demonstrated in this study. For high buildings with more than 10 floors, the combination of UAV and TLS technologies proves to be more reasonable and effective.

For buildings with 10 floors or fewer, combining UAV and terrestrial photogrammetry (TP) technologies would be more reasonable and effective. The reason is that terrestrial photogrammetry technology is more cost-effective than lidar scanning but provides comparable accuracy. However, the limitation of this method is that the data collection process outside the field is longer, and the distance from the terrestrial photogrammetry image capture point to the object must be calculated reasonably to obtain dense and accurate point clouds.

4. Conclusion

This study has proposed a comprehensive process for constructing complete 3D models for several distinctive construction projects in coastal urban areas. The overall procedure is proposed with the integration of geospatial technologies, including UAV aerial photography, ground-based photography, and terrestrial LiDAR scanning, to build highly accurate 3D models for the research area, which is suitable for the current technological and human resource conditions in Vietnam.

The findings of this study recommend that for high buildings with more than 10 floors, the combination of UAV and TLS technology proves to be more reasonable and effective. Meanwhile, for buildings with 10 floors or fewer, integrating UAV technology with terrestrial photogrammetry (TP) would be more reasonable.

In our study, we constructed 3D building models using point clouds generated from data collected by low-cost DJI Phantom 4 Pro drone equipment and the Sony 7R ground-based camera, and the FARO FOCUS3D X130 TLS. The point clouds derived from the Sony and FARO FOCUS3D X130 TLS devices were dense and provided high resolution; however, they had limitations in coverage, especially for building roofs. On the other hand, the point clouds generated by the UAS presented a comprehensive building model, albeit with lower resolution. The integration of these technologies is a trend that future research in Vietnam is likely to increasingly adopt.

Author contribution statement: Generating the research idea; statement of the research problem; analysis of research results and data preparation; wrote the draft manuscript: H.T.T.L.; Analyzed and interpreted the data, wrote the draft manuscript: H.T.T.L.

Competing interest statement: The authors declare no conflict of interest.

References

1. Bouziani, M.; Chaaba, H.; Ettarid, M. Evaluation of 3D building model using terrestrial laser scanning and drone photogrammetry. *Int. Arch. Photogramm. Remote Sens. Spatial Inf. Sci.* **2021**, *XLVI-4/W4-2021*, 39–42.
2. Nex, F.; Remondino, F. UAV for 3D mapping applications: a review. *Appl. Geomatics* **2013**, *6(1)*, 1–15.
3. Böhm, J.; Brédif, M.; Gierlinger, T.; Krämer, M.; Lindenberg, R.; Liu, K.; Michel, F.; Sirmacek, B. Te IQmulus urban showcase: automatic tree classification and identification in huge mobile mapping point clouds. *Int. Arch. Photogramm. Remote Sens. Spatial Inf. Sci.* **2016**, *XLI-B3*, 301–307.
4. Kaartinen, H.; Hyypä, J.; Kukko, A.; Jaakkola, A.; Hyypä, H. Benchmarking the performance of mobile laser scanning systems using a permanent test field. *Sensors* **2012**, *12(12)*, 12814–12835.
5. Früh, C.; Zakhor, A. An automated method for large-scale, ground-based city model

- acquisition. *Int. J. Comput. Vision* **2004**, *60*(1), 5–24.
6. Tack, F.; Buyuksalih, G.; Goossens, R. 3D building reconstruction based on given ground plan information and surface models extracted from spaceborne imagery. *ISPRS J. Photogramm. Remote Sens.* **2012**, *67*, 52–64.
 7. Colomina, I.; Molina, P. Unmanned aerial systems for photogrammetry and remote sensing: A review. *ISPRS J. Photogramm. Remote Sens.* **2014**, *92*, 79–97.
 8. Fischer, A.; Kolbe, T.H.; Lang, F.; Cremers, A.B.; Förstner, W.; Plümer, L.; Steinhage, V. Extracting buildings from aerial images using hierarchical aggregation in 2D and 3D. *Comput. Vision Image Understanding* **1998**, *72*(2), 185–203.
 9. Stilla, U.; Soergel, U.; Toennessen, U. Potential and limits of InSAR data for building reconstruction in built-up areas. *ISPRS J. Photogramm. Remote Sens.* **2003**, *58*(1-2), 113–123.
 10. Wang, Y.; Huang, X.; Gao, M. 3D model of building based on multi-source data fusion. *Int. Arch. Photogramm. Remote Sens. Spatial Inf. Sci.* **2022**, *XLVIII-3/W2-2022*, 73–78. <https://doi.org/10.5194/isprs-archives-XLVIII-3-W2-2022-73-2022>.
 11. Whitehead, K.; Hugenholtz, C.H. Remote sensing of the environment with small unmanned aircraft systems (UASs), part 1: A review of progress and challenges. *J. Unmanned Vehicle Syst.* **2014**, *2*, 69–85. <https://doi.org/10.1139/juvs-2014-0006>.
 12. Ha, L.T.T.; Long, N.Q. Combination of UAV image and terrestrial photogrammetry to build 3D geospatial data for smart cities. *J. Hydro-Meteorol.* **2013**, *749*, 21–31. [https://doi.org/10.36335/VNJHM.2023\(749\).21-31](https://doi.org/10.36335/VNJHM.2023(749).21-31).
 13. Barnhart, T.B.; Crosby, B.T. Comparing two methods of surface change detection on an evolving thermokarst using high-temporal-frequency terrestrial laser scanning, Selawik River. *Alaska Rem. Sens.* **2013**, *5*, 2813–2837. <https://doi.org/10.3390/rs5062813>.
 14. Erdélyi, J.; Kopác'ik, A.; Lipták, I.; Kyrinovic, P.; Automation of point cloud processing to increase the deformation monitoring accuracy. *Appl. Geomat.* **2017**, *9*(2), 105–113. <https://doi.org/10.1007/s12518-017-0186-y>.
 15. Fan, J.; Wang, Q.; Liu, G.; Zhang, L.U.; Guo, Z.; Tong, L.; Peng, J.; Yuan, W.; Zhou, W.; Yan, J.; Perski, Z.; Sousa, J. Monitoring and analyzing mountain glacier surface movement using SAR data and a terrestrial laser scanner: A case study of the Himalayas North Slope Glacier Area. *Rem. Sens.* **2019**, *11*(6), 625. <https://doi.org/10.3390/rs11060625>.
 16. Xu, Z.; Xu, E.; Wu, L.; Liu, S.; Mao, Y. Registration of terrestrial laser scanning surveys using terrain-invariant regions for measuring exploitative volumes over open-pit mines. *Rem. Sens.* **2019**, *11*(6), 606. <https://doi.org/10.3390/rs11060606>.
 17. Harmening, C.; Neuner, H. A spatio-temporal deformation model for laser scanning point clouds. *J. Geod.* **2020**, *94*, 1–25. <https://doi.org/10.1007/s00190-020-01352-0>.
 18. Whitehead, K.; Hugenholtz, C.H. Remote sensing of the environment with small unmanned aircraft systems (UASs), part 1: A review of progress and challenges. *J. Unmanned Vehicle Syst.* **2014**, *2*, 69–85. <https://doi.org/10.1139/juvs-2014-0006>.
 19. Sayab, M.; Aerden, D.; Paananen, M.; Saarela, P. Virtual structural analysis of Jokisivu open pit using “structure-from-motion” unmanned aerial vehicles (UAV) photogrammetry: Implications for structurally-controlled gold deposits in Southwest Finland. *Rem. Sens.* **2018**, *10*, 1–17. <https://doi.org/10.3390/rs10081296>.
 20. Chhatkuli, S.; Satoh, T.; Tachibana, K. Multi sensor data integration for an accurate 3D model generation. *Int. Arch. Photogramm. Remote Sens. Spatial Inf. Sci.* **2015**, *XL-4/W5*, 103–106. <https://doi.org/10.5194/isprsarchives-XL-4-W5-103-2015>.
 21. Hannes, P.; Martin, S.; Henri, E. A 3-D model of castle Landenberg (CH) from combined photogrammetric processing of terrestrial and UAV based images. *Int.*

Arch. Photogramm. Remote Sens. Spatial Inf. Sci. **2008**, *37*, 93–98.

22. Long, V.P.; et al. Flying and taking photos with an unmanned aerial vehicle (UAV) creates a 3-dimensional (3D) spatial map. *J. Surv. Mapp. Sci.* **2017**, *31*, 23–28.
23. Duy, B.T. Constructing a three-dimensional model of Hanoi National University using handheld cameras and its applications in this three-dimensional model, Project code: QC.05.02. Summary report of the national university-level scientific research project conducted by the University of Technology and Management. 2011, pp. 60.
24. Hu, Z. ICP algorithm for 3D surface registration. *Highlights Sci. Eng. Technol.* **2022**, *24*, 94–98.